OPEN

PRS GLOBAL OPEN

ORIGINAL ARTICLE
Research

Lymph Node Inclusion in a Modified Osteomyocutaneous Allograft for Vascularized Composite Allotransplantation: Establishment and Feasibility Assessment in a Pig Model

Stefanie Hirsiger, MD*
Ioana Lese, MD*
Isabel Arenas Hoyos, MD*†
Cédric Zubler, MD‡
David Haberthür, PhD‡
Ruslan Hlushchuk, MD‡
Valentin Djonov, MD‡
Yara Banz, MD, PhD§
Ana Macek, MD¶
Hendrik von Tengg-Kobligk, MD¶
Daniela Casoni, VMD, PhD†
Robert Rieben, PhD†
Radu Olariu, MD, PhD*

Background: Representative translational animal models play a key role in vascularized composite allotransplantation (VCA) research. A composite porcine hindlimb flap, previously described, is a relevant preclinical model. However, its bulkiness and the absence of critical immunologic tissues make it less suitable for investigating the unique immunologic features of VCA. We aimed to further develop this model by reducing its bulkiness and by including donor-draining lymph nodes.

Methods: We conducted an anatomic study by harvesting 11 porcine osteomyocutaneous flaps (4 conventional and 7 modified techniques), which were characterized by computed tomography. Furthermore, 8 allotransplantations were performed in Swiss landrace pigs. After the procedure, animals were assigned to a model development and control group (N = 4 per group). No immunosuppression was given, and animals were followed up until grade 3 rejection.

Results: With the modified technique, the flap weight was significantly reduced with a mean weight of 831 g, corresponding to 1.8% total body weight versus 1710 g in the conventional technique, representing 4.2% of total body weight ($P < 0.0001$). The muscle/bone ratio was reduced from 8.24 (conventional) to 2.92 (modified), ($P = 0.03$). Histologically, graft-draining lymph nodes showed typical changes related to rejection and no signs of ischemia after in vivo transplantation.

Conclusions: By modifying the surgical technique, the bulkiness of the flap was markedly reduced, without impairing its vascularization and reliably including vascularized graft-draining lymph nodes. Our modified VCA model in the pig presents distinct advantages for surgery as well as immunologic analysis, warranting a large-scale use for experimental reconstructive transplantation studies. *(Plast Reconstr Surg Glob Open 2024; 12:e6296; doi: 10.1097/GOX.0000000000006296; Published online 11 November 2024.)*

*From the *Department of Plastic and Hand Surgery, Inselspital University Hospital, University of Bern, Bern, Switzerland; †Department for BioMedical Research, University of Bern, Bern, Switzerland; ‡Institute of Anatomy, University of Bern, Bern, Switzerland; §Institute of Pathology, University of Bern, Bern, Switzerland; and ¶Department of Diagnostic, Interventional and Paediatric Radiology, Inselspital University Hospital, University of Bern, Bern, Switzerland.*

Received for publication March 15, 2024; accepted September 11, 2024.

Presented at the 20th Congress of the European Society for Organ Transplantation in Milan, Italy, August 2021.

Drs. Hirsiger, Lese, and Arenas Hoyos contributed equally to this work.

Copyright © 2024 The Authors. Published by Wolters Kluwer Health, Inc. on behalf of The American Society of Plastic Surgeons. This is an open-access article distributed under the terms of the Creative Commons Attribution-Non Commercial-No Derivatives License 4.0 (CCBY-NC-ND), where it is permissible to download and share the work provided it is properly cited. The work cannot be changed in any way or used commercially without permission from the journal.

DOI: 10.1097/GOX.0000000000006296

INTRODUCTION

Clinical vascularized composite allotransplantation (VCA) has risen in interest and development in the last years[1] with more than 167 transplants performed worldwide.[2–4] However, wide acceptance of VCA is hindered by severe side effects associated with systemic immunosuppression.[1,5,6] To overcome the problems associated with systemic immunosuppression, local delivery of immunosuppressive drugs has been investigated as a possibility to induce graft survival with reduced off-target effects.[7–9] Although rodent experiments show highly promising results,[10–13] further evaluation in a large-animal model with more similarities to the human immunologic system is

Disclosure statements are at the end of this article, following the correspondence information.

Related Digital Media are available in the full-text version of the article on www.PRSGlobalOpen.com.

necessary before local immunosuppression protocols can be used in the clinical setting.[14] The swine seems to fulfill the criteria needed for the results to be reproducible in humans.[15] Swine VCA models described in the literature range from radial forelimb osteomyocutaneous flaps and forelimb transplantation to heterotopic hindlimb models, each with advantages and disadvantages. Although the radial forelimb osteomyocutaneous flap lacks articular cartilage,[16] the forelimb transplantation model, where the medial digit of the animal is included in the graft[17] or the entire forelimb up to the level of the radius and ulna is included,[18] interferes with the well-being of the animals as the postoperative ambulation is limited due to the full-length cast. To overcome these drawbacks, other groups have envisioned hindlimb transplantations containing different tissue types of VCA that would allow the animals to ambulate freely.[19–22] Nonetheless, the bulkiness of the described models, especially in the heterotopic technique with the graft placed in an abdominal pocket, might compress the vascular anastomoses and lead to technical failures. Also, the relationship of different components in the allograft, especially skin to muscle, is much different from that of a clinical allograft (hand or face transplant), leading to potential differences in immunologic response.

Common to all swine VCA models described in the literature is the lack of draining lymph nodes in the transplant. Lymph nodes play a crucial role in the trafficking of immune cells between the graft and the host during rejection/tolerance.[23,24] Our group first described a lymph node-including VCA model in rodents.[25] In line with findings from solid organ transplantation,[26] we demonstrated that the presence of donor-draining lymph nodes within the osteomyocutaneous graft was linked to delayed graft rejection. This delay was facilitated by the promotion of lymphangiogenesis and an increase in chimerism levels.[27] Nevertheless, the exploration of the role of graft-draining lymph nodes is not well addressed in the VCA literature, potentially also due to the lack of adequate large-animal models. Considering all these perceived drawbacks, we aimed to further develop and optimize a heterotopic VCA model in pigs that is less bulky, has a component distribution more similar to the clinically used transplants, and includes graft-draining lymph nodes.

Takeaways

Question: How can we provide good translational models to accelerate the clinical application of experimental findings in vascularized composite allotransplantation (VCA)?

Findings: We have developed a reliable heterotopic VCA model in pigs with reduced bulkiness and inclusion of graft-draining lymph nodes. We have tested the model anatomically and in experimental VCA.

Meaning: Easier, more reliable, and more clinically resembling VCA models in large animals can greatly facilitate further translational VCA research.

MATERIALS AND METHODS

All animal experiments were approved by the Bern Cantonal Animal Experimentation Committee in Switzerland (license number BE48/19).

Anatomic Study

We developed a model through an anatomical study, harvesting 11 porcine osteomyocutaneous flaps: 4 using the conventional method and 7 with a modified technique (details provided later). The pigs, previously used in unrelated research, had their limbs amputated before euthanasia. The flaps were weighed and analyzed using conventional computer tomography (CT) (9 flaps: 4 conventional and 5 modified) and micro-CT (2 flaps, both modified). Further details on CT volumetry and micro-CT angiography are available in Supplemental Digital Content 1 and 2. (**See appendix, Supplemental Digital Content 1,** which displays volumetry calculation based on conventional CT. An example of a CT volumetry showing the different structures of a flap from the modified technique. Skin and subcutaneous tissue are depicted in red. Lymph nodes, muscle, and bone are depicted in different green tones, **http://links.lww.com/PRSGO/D603**.) (**See appendix, Supplemental Digital Content 2,** which displays supplement materials and methods, **http://links.lww.com/PRSGO/D604**.)

Animal Experiment

A total of 8 heterotopic transplantations were performed in 12 (4 donors and 8 recipients) swine leucocyte antigen–mismatched Swiss landrace pigs. Recipient animals were assigned to a model establishment (N = 4 animals) and a control group (N = 4 animals). Control animals were followed up until at least grade 3 rejection, which was confirmed histologically and classified according to the BANFF system.[28,29] (**Supplemental Digital Content 2, http://links.lww.com/PRSGO/D604**). No immunosuppressive treatment was given in this group.

Donor Pig Surgery

Anesthesia and Monitoring

Previous to the sedation of the animal, a peripheral venous catheter was placed to induce general anesthesia intravenously. Tracheal intubation was then performed. Central venous and arterial catheters were placed together with a transabdominal bladder catheter to improve monitoring. Depth of anesthesia and adequacy of nociception were continuously monitored by electroencephalogram and tracking of nociceptive withdrawal reflexes. Additional analgesia was provided by an epidural block with ropivacaine and methadone. (**See appendix, Supplemental Digital Content 3,** which displays anesthesia and monitoring, **http://links.lww.com/PRSGO/D605**.)

Osteomyocutaneous Limb Allograft Harvest

The femoral artery and its perforators in the anteromedial thigh region were located and marked using a handheld Doppler. Based on the latter, a ~150 cm^2 lentil-shaped skin paddle was defined. [**See appendix, Supplemental Digital Content 4,** which displays the marking of the skin

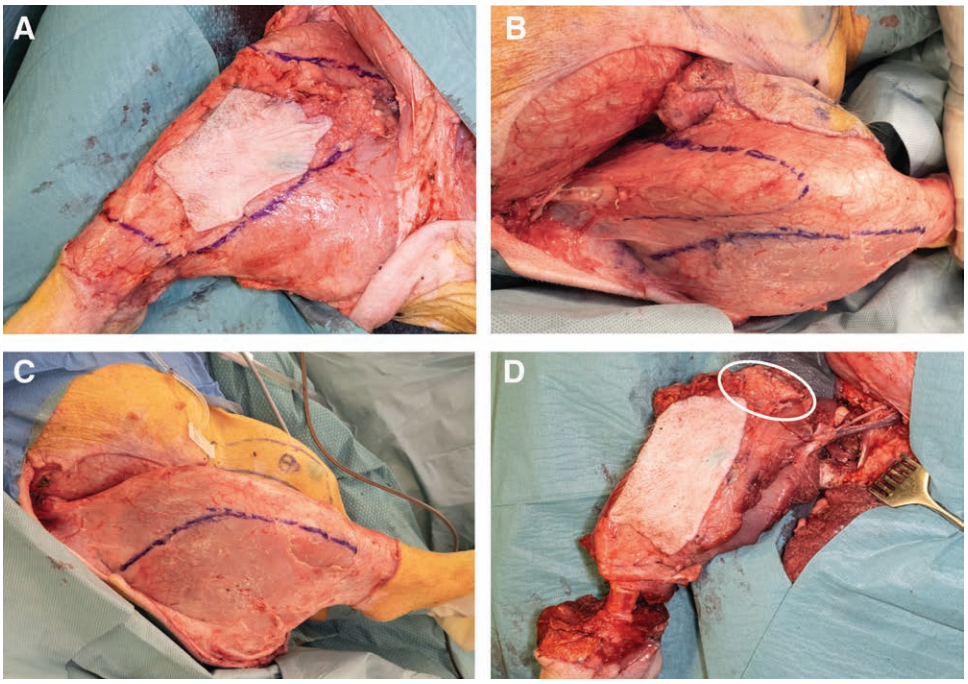

Fig. 1. Steps of the dissection. A, Skin paddle in the medial thigh and inguinal region. B and C, Marking of muscle resection to reduce bulk. D, Isolated femoral pedicle, inclusion of draining lymph nodes marked with a white ellipse.

paddle and lymph nodes. A, Skin paddle marked based on the perforator and femoral artery on the medial right thigh. B, Clinical image showing indocyanine green (ICG). C, Near-infrared fluorescence imaging (NIRFI) in an overlay manner, **http://links.lww.com/PRSGO/D606**.] To localize graft-draining lymph nodes, ICG was injected on the planned skin paddle (**Supplemental Digital Content 4B, http://links.lww.com/PRSGO/D606**). The draining lymphatic vessels and lymph nodes were identified by NIRFI using the Visionsense Camera (Medtronic, Minneapolis, Minn.) (**Supplemental Digital Content 4C**, **http://links.lww.com/PRSGO/D606**). If necessary, the skin paddle was adjusted to cover the lymphatic draining area optimally.

Previous disinfection and sterile surgical draping, the skin was incised on the markings with a scalpel. Once the muscle fascia was reached, resorbable stitches were used in the distal part to prevent shearing and, thus, devascularization of the skin paddle. Lymph nodes, easily found based on the ICG dye, were dissected en bloc and marked with a nonresorbable stitch. The dissection was carried down through the connective tissue plane to the inguinal ligament. The femoral artery and vein were carefully dissected, proximally up under the inguinal ligament and distally to the level of the suprageniculate branches. To prepare the rest of the graft, the skin of the rest of the thigh circumference was removed (Fig. 1A). The cranial tibial muscle, digital extensors, peroneus muscles, and flexor muscles were cut using electrocautery. The saphenous artery and veins, as well as the anterior and posterior tibial arteries, were ligated. An oscillating saw was used for the osteotomies (mid-femur and mid-tibial/fibular), and the bone edges of the graft were smoothened.

The flap now contained the skin paddle, knee joint, distal femur and proximal tibia, and a large muscle bulk. To minimize the impact on the recipient's morbidity, we implemented several modifications to decrease the flap size.

First, to diminish blood loss, we performed the osteotomies only immediately before the flap ischemia. As bleeding from the marrow remained profuse and flushed away bone wax, we tailored plugs from the discarded distal tibial cortex to fit the medullary canals of the femur and tibia in the flap.

Second, to reduce bulkiness, we resected several muscles. The rectus femoris, tensor fascia latae, vastus lateralis, and medialis (partial) as well as the biceps femoris (partial), semimembranosus, semitendinosus, and adductor muscles (partial) were removed from the thigh, whereas the gastrocnemius muscle was excised from the lower leg (Fig. 1B, C). The popliteal artery was carefully protected, and the sciatic nerve was cut distally immediately after its separation in the tibial and peroneal nerves. A more detailed explanation of the debulking process can be found in Supplemental Digital Content 5. [**See appendix, Supplemental Digital Content 5,** which displays steps in muscle debulking. A, After the identification and dissection of the femoral A–V bundle the rectus femoris and vastus medialis (partial) are incised from the medial femoral side and detached distally from the quadriceps tendon. B, Afterward, the dissection turns on the lateral side, and the tensor fasciae latae muscle is detached en bloc with the rectus femoris and vastus lateralis (partial). The vastus intermedius is kept entirely. The lateral muscular septum is opened. C, Now the biceps femoris muscle

is incised distally and the biceps femoris muscle and the smaller semitendinosus and semimembranosus muscles are retracted proximally. Care must be taken to identify and protect the main branch of the sciatic nerve while cutting its muscular branches. D, After the incision of the lower leg muscles has been performed at the site of the osteotomy, the lateral muscle debulking is completed. E, Now, dissection is continued on the medial side, and the adductor muscles are cut distally close to the insertion but leaving a distal muscle cuff to protect the femoral vascular bundle. F, The obturator nerve and branches of the deep femoral artery and vein need to be identified, ligated, and cut. Now, the dissection is ready for the femoral and tibiofibular osteotomies to be performed, leaving the debulked osteomyocutaneous flap on its femoral pedicle, **http://links.lww.com/PRSGO/D607**.] The flap now contains the representative structures of a limb allotransplant, with a smaller muscle bulk and including graft-draining lymph nodes (Fig. 1D).

The pedicle was not clamped until the vessels of the recipient pig were ready for the anastomosis. Although the first flap was transplanted to the recipient, the second flap was raised on the contralateral limb by a second surgical team. The donor animal was euthanized directly after the second flap ischemia by intravenous injection of 100 mg/kg pentobarbital. Flat electroencephalogram and asystole (electrical silence in the electrocardiogram) confirmed the pigs' death.

Recipient Pig Surgery

For the recipient, in addition to the anesthesiologic intervention described earlier, cefuroxime was given at induction of general anesthesia and 6 hours later. The pig was installed as described for the donor. A straight incision of about 20 cm in length was made in the inguinal fold. Dissection was carried down to the vessels, which were carefully dissected as described for the donor. To accommodate the graft, a subcutaneous pocket was created, cranially reaching over the most caudal ribs and dorsally over the lateral spinal processes.

The graft was then disconnected from the donor by division of the pedicle, weighed and flushed with 200–250 mL Custodiol HTK solution (Dr. Franz Köhler Chemie GmbH, Bensheim, Germany) until clear fluid drained through the vein. (**See appendix, Supplemental Digital Content 6,** which displays steps of graft insertion. A, Vascular composite allograft of forelimb after complete dissection. B, Femoral vessel anastomosis in recipient pig, inguinal incision. C, A definitive clinical image after transplantation with a viable skin paddle and pain catheter is in place, **http://links.lww.com/PRSGO/D608**.) The musculature of the flap was sutured to the abdominal wall (but not to the hindlimb). The pedicle of the recipient was then transected as distally as possible. The distal end of the vessel was clipped, leaving the limb perfused only by collaterals. The arterial anastomosis was performed by standard microsurgical technique, and the venous anastomosis by using a coupling device under a microscope. (**Supplemental Digital Content 6B, http://links.lww.com/PRSGO/D608**). The flap's smaller size allows the skin paddle to be easily positioned dorsolaterally, thereby facilitating observation in a standing or lying pig.

As a final step, the skin on the flank of the recipient that lies over the graft is excised, the flap skin paddle exteriorized, and the skin sutured with resorbable material. A small indwelling pain catheter was placed in the wound, and additional peri-incisional ropivacaine 0.75% (maximum of 4 mg/kg) was injected at closure and repeated in the first 48 hours (**Supplemental Digital Content 6C, http://links.lww.com/PRSGO/D608**). At the end of the surgery, a port-a-cath was implanted via a midline incision for the central venous and arterial lines (see above) and an additional dorsal incision for pouch placement.

Timing

During the surgical procedure, the timing of the following parts of the procedure was recorded (in minutes):

- Graft harvesting time (donor): From skin incision to complete freeing of the flap on the vascular pedicle only.
- Site preparation (recipient): From skin incision to end of preparation of tissue pocket and recipient vessels for anastomosis.
- Transplantation time (recipient): From the start of the inset of the donor graft in the recipient bed until skin suture (includes anastomoses).
- Warm ischemia (donor graft): From pedicle clamping until re-establishment of arterial and venous flow (venous anastomosis was performed first).

Statistical Analysis

All values are given as mean ± SD. Statistical analysis was performed with Prism 9.4.0 (GraphPad Software). The Student *t* test or the Mann–Whitney test, depending on the distribution of the data, was used for the continuous variables (weight, volumes, and times).

RESULTS

Anatomic Study

The data from the anatomical study are shown in Supplemental Digital Content 7. [**See table, Supplemental Digital Content 7,** which displays the summary of total body weight (TBW) versus graft weight in the modified and conventional groups, **http://links.lww.com/PRSGO/D609**.] The mean weight of the flaps with the conventional technique was 1710 g (range 1564–1961 g), corresponding to a mean of 4.2% ± 0.38% of TBW. The flap weight was significantly reduced with the modified technique with a mean weight of 831 g (range 538–1080 g), corresponding to 1.8% ± 0.18% TBW ($P < 0.0001$).

Conventional CT Volumetry

The volumetry measurements for the 9 flaps that underwent conventional CT-based volumetry are summarized in Supplemental Digital Content 8. (**See table, Supplemental Digital Content 8,** which displays the summary of conventional CT volumetry in the modified and conventional grafts, **http://links.lww.com/PRSGO/D610**.)

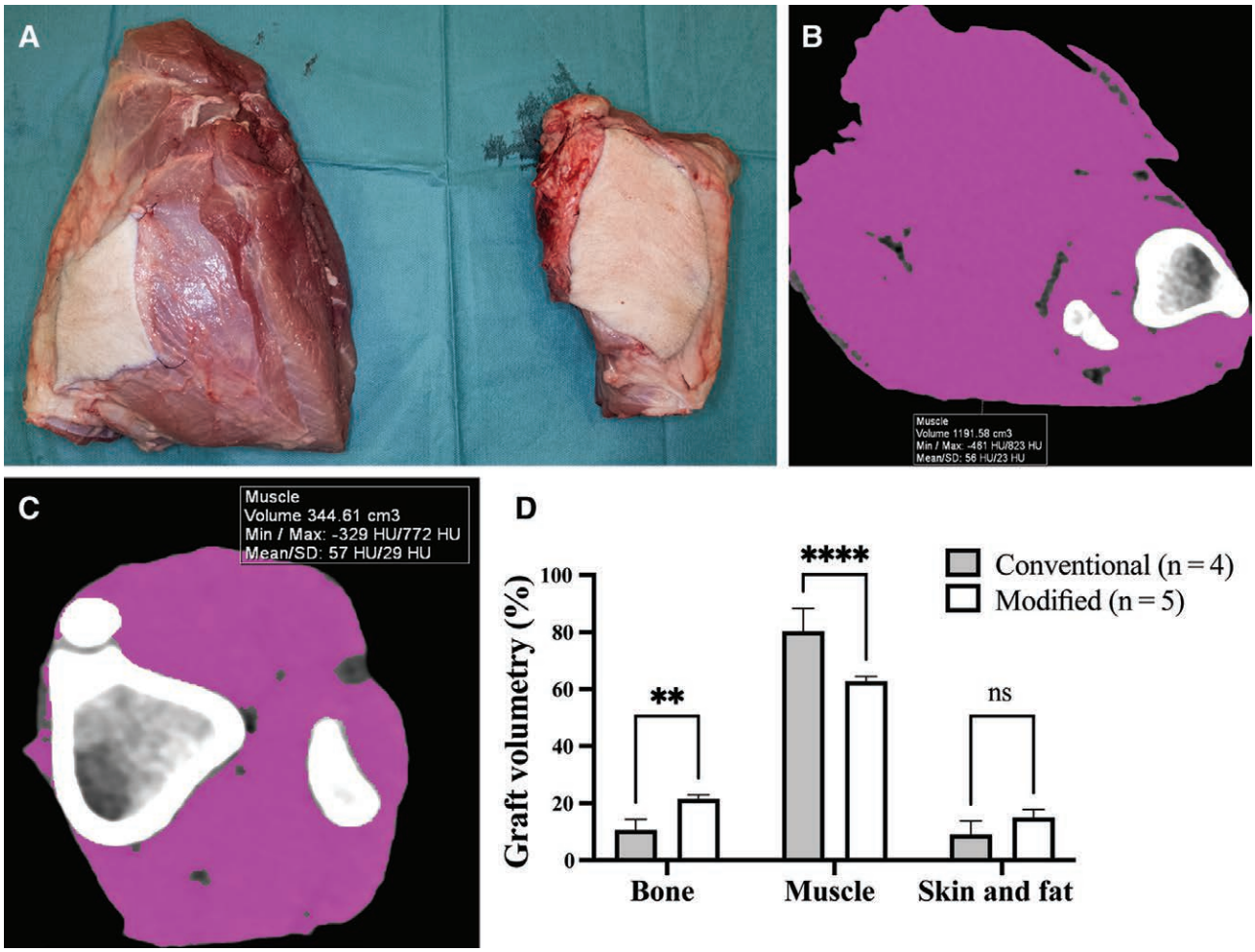

Fig. 2. Clinical, radiographic, and volumetric comparison of the conventional and modified model. A, Comparison of the clinical graft appearance of the conventional (left) and modified (right). CT volumetry of the (B) conventional and (C) modified techniques. D, Volumetry quantification in bone, muscle and skin/fat (**$P < 0.01$, ****$P < 0.0001$, n.s: not significant).

The muscle-to-bone ratio was significantly reduced in the modified technique (2.92 ± 0.14) compared with conventional flap raising (8.24 ± 2.71, $P = 0.03$). Also, the relative volume of skin and fat was significantly increased in the modified group (15.01% ± 2.80%) compared with the conventional technique (8.89% ± 4.39%, $P = 0.04$) (Fig. 2).

Micro-CT angiography revealed complete vascularization in all tissues included in the modified flap. Vascularization of the lymph nodes was clearly visible (Fig. 3).

Animal Experiment

The animals in the model development group were used to develop, assess, and fine-tune logistical, anesthesiologic, and surgical methods. In case of a successful surgery and no postoperative complication, the animals were included in the control group. In the model development groups, we witnessed some complications. In 2 animals, venous insufficiency was noticed. In 1 animal, ~4 hours postoperatively, associated with massive bleeding, leading to euthanasia per protocol. In the other animal, venous insufficiency was noted on postoperative day 1, and the animal was euthanized. The protocol was amended to increase awareness of positioning of the venous anastomosis with respect to the flap and the arterial anastomosis to prevent kinking and pressure of the flap and/or artery on the vein with subsequent mobilization. In 1 pig, the arterial anastomosis ripped soon after waking up, leading to immediate euthanasia. This complication was deemed to be a result of suboptimal flap fixation of a possibly too-large flap combined with massive agitation of the animal after extubation. The surgical protocol was amended to include at least 4 points of fixation to the abdominal wall with deep Vicryl 0 sutures, increased awareness for flap debulking as described in the methods section, and the anesthesiologic protocol was amended to include epidural blocks in the recipients as well.

In the control group (N = 4), all transplantations were successful, and the animals showed clinical rejection as expected around 6–8 days with a median survival time of 7.5 days (Fig. 4).

Timing

During the total of 8 transplantations, the recorded times for the procedure steps were:

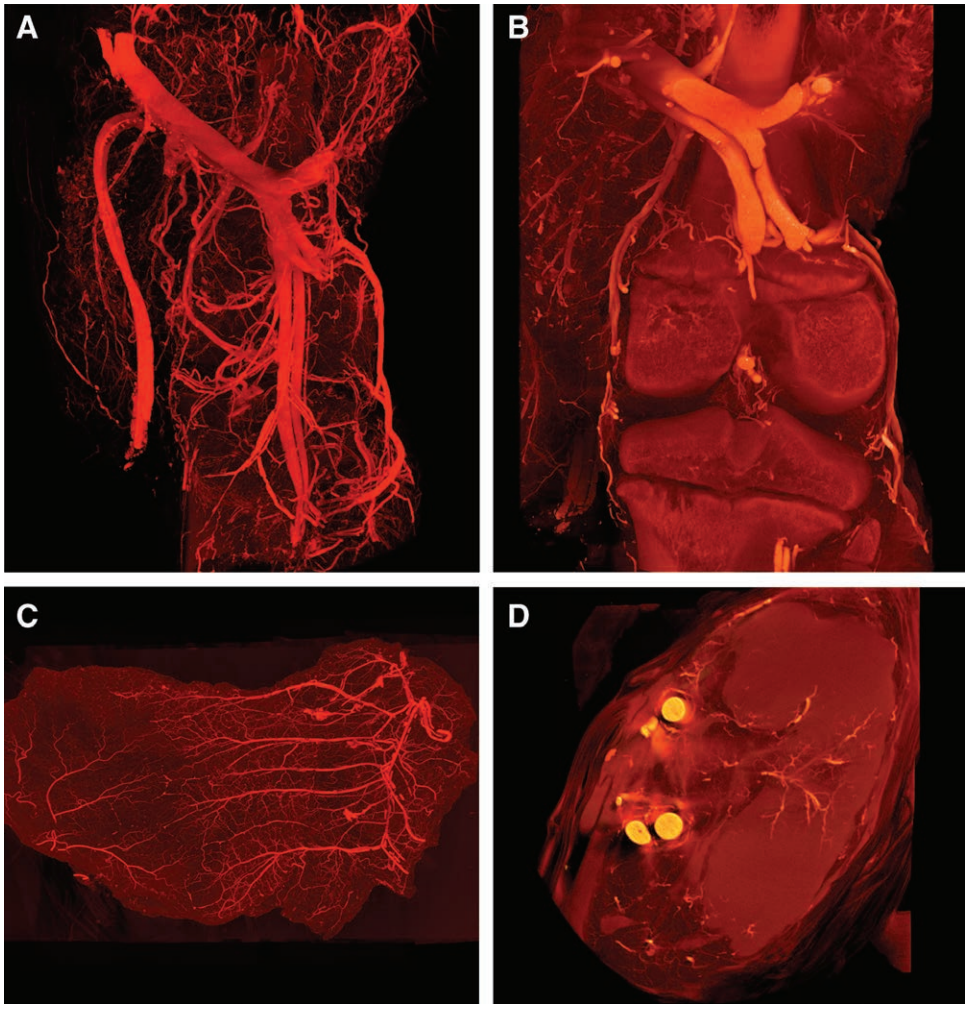

Fig. 3. Micro-CT angiography of the allograft. A, Overview of the whole specimen (15×10×9 cm) vascularization. B, Bone marrow vascularization. C, Skin- and fat-pad scans (14×8 × 2.2 cm) showing skin-pad vascularization (left) and the fat pad containing the lymph nodes (right). D, High-resolution reconstruction of a single lymph node (1.5 × 0.9).

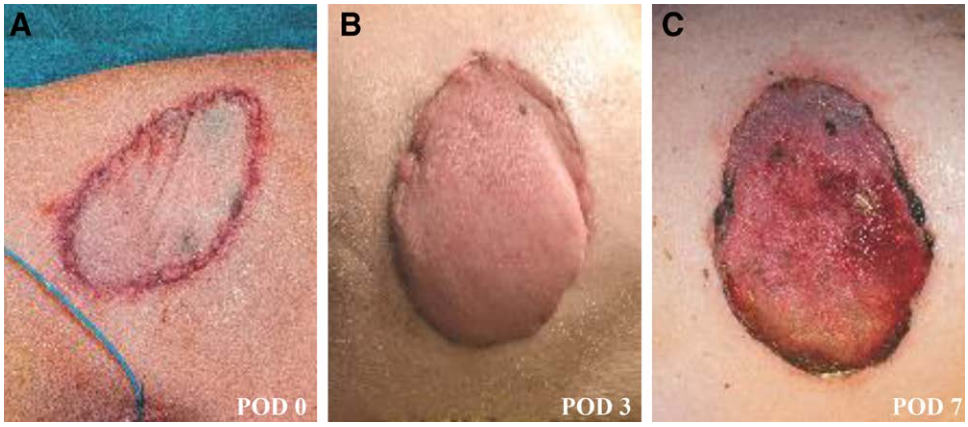

Fig. 4. Macroscopic graft follow-up. Representative clinical images of the monitoring skin island at (A) POD 0 (grade 0 rejection), (B) POD 3 (grade I rejection), and (C) POD 7 (grade III rejection). POD, post-operative day.

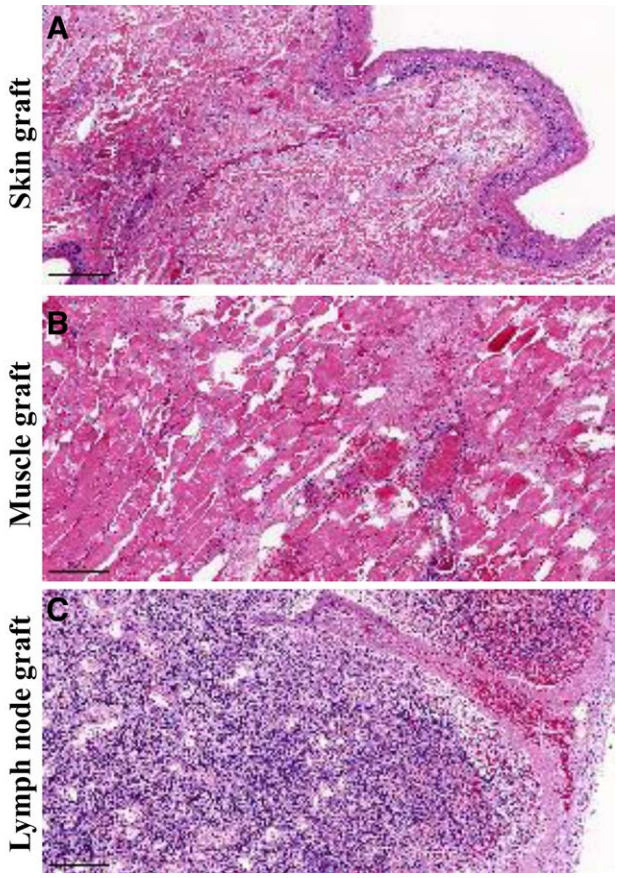

Fig. 5. Histopathologic Banff evaluation of skin grafts at endpoint. Representative images from hematoxylin and eosin–stained histological specimens of (A) skin, (B) skeletal muscle, and (C) lymph node.

- Graft harvesting time 102.75 ± 22.78 minutes.
- Site preparation (recipient) 37.75 ± 11.16 minutes.
- Transplantation time (recipient) 118.13 ± 18.22 minutes.
- Warm ischemia (donor graft) 65.5 ± 11.11 minutes.

A clear trend for faster surgery was visible, especially regarding graft harvesting time, highlighting the impact of the learning curve for this procedure. [**See appendix, Supplemental Digital Content 9**, which displays the evolution of surgical timing parameters over time. Linear chart (with trend lines) of the evolution of procedure times for different surgical steps. The animals are ordered by date of surgery (lower numbers equal surgery further in the past), **http://links.lww.com/PRSGO/D611**.]

Immunohistochemistry

The histopathologic analysis of the different samples taken from the grafts at endpoint (clinical grade III rejection in the skin) showed typical changes of rejection (Fig. 5). At the endpoint, donor-draining lymph nodes in the explanted graft were identified using the nonresorbable stitch marker placed previously. Lymph nodes showed no signs of ischemia and the rejection changes

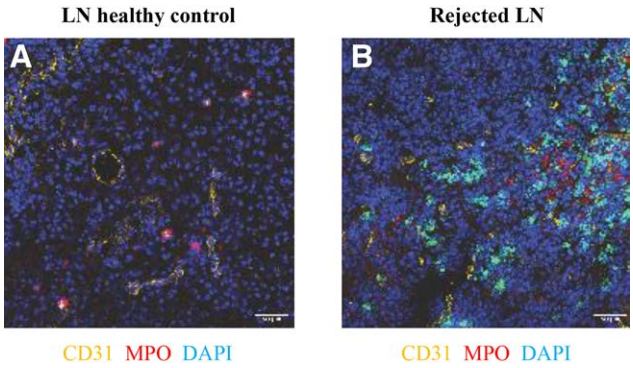

Fig. 6. Immunofluorescence staining of graft-draining lymph nodes upon rejection. Representative immunofluorescence staining of lymph nodes from (A) healthy-naive animals (control) and (B) donor-draining lymph nodes upon allograft rejection. Samples were stained for cell nuclei (DAPI-blue), endothelial cells (CD31-yellow) and neutrophils (MPO-red). DAPI, 4′,6-diamidino-2-phenylindole; MPO, myeloperoxidase.

in the lymph nodes paralleled those in skin and muscle. Additionally, there was increased neutrophil infiltration and vascularity in the donor-draining lymph nodes from the graft, as assessed by immunofluorescence, confirming the presence of an immunologically active structure up to the endpoint (Fig. 6).

DISCUSSION

Despite the rapid progress in human VCA in recent years, widespread use is hampered by the slow progress in the development of immunosuppression regimens with reduced off-target effects.[1,5,6] Although this has been extensively studied in rodents, large-animal models are crucial in addressing these unresolved queries. Because the few described models in the literature present some drawbacks,[14] we have envisioned a modified technique of a heterotopic VCA model in pigs where we could address some of the main concerns.

Although the main idea behind the various modifications of the described orthotopic forelimb VCA model[16,17,30] was to test the flap's function at an endpoint, the only functional outcome that could be assessed was joint stability by manual manipulation of the joint. However, innervation and sensation could also be theoretically tested. Fries et al[18] described their pilot study using a complete orthotopic forelimb VCA model in pigs. Even though the possibility of assessing the graft's outcomes in terms of motor and sensitive function seems promising, the cast needed postoperatively, and the imaginable postoperative ambulation problems represent significant impediments of this model regarding animal welfare and increased regulatory burden. Therefore, a model where ambulation is not impaired would be highly desirable. Thus, a heterotopic model is likely to be preferred to not submit the animals to unnecessary stress.

The first skin-including heterotopic VCA model in pigs was described by Mathes et al.[20] Skin is considered the most antigenic structure out of all the relevant structures

and tissue types of VCA.[31–33] There has been a continuous debate regarding the need for higher doses of immunosuppressive therapy compared with solid organ transplantation,[34] but a definite conclusion has yet to be drawn. However, the skin is a major component of hand and face transplantation and should be the main focus in all preclinical models. In our study, the modified technique entails less muscle, whereas the skin component is better represented. As described in the modifications by Kuo et al[22] and Ibrahim et al,[21] we have also placed the skin island on the dorsolateral region of the abdominal wall to make graft monitoring easier. To address the increased abdominal wall girth due to the bulkiness of the graft, we have envisioned a model with less muscle mass but without compromising the perfusion of the graft's components. Our vascular anastomosis technique is similar to the improvements implemented by Ibrahim et al[21] during their study because it shortens the microsurgical time of the procedure: the artery is sutured end-to-end to the femoral artery stump in a classical manner with stitches, although the vein is anastomosed with a coupler to the femoral vein. However, our mean warm ischemia time was shorter than what the authors described in their article: 65.5 minutes, compared with 78 minutes. Moreover, even though we could not find values for graft harvesting or transplantation time in previous literature, in our study, we saw a clear trend of shorter times toward the end of the series, most probably explained by the learning curve.

As demonstrated before, the presence of draining donor lymph nodes within the VCA allograft delays the onset of acute rejection.[27] Although there is only one VCA model with graft-draining lymph nodes described in the rat,[25] we aimed to develop a similar pig model. Therefore, the presented model includes the draining lymphatic vessels and lymph nodes that were visualized intraoperatively by NIRFI. Moreover, the vascularization and perfusion of the lymph nodes were confirmed with both micro-CT angiography and histologically at the end of the in vivo experiments, where the histopathologic analysis of the lymph nodes showed no signs of ischemia.

However, limitations persist; due to the VCA's heterotopic position, functional motor, and sensory outcomes cannot be assessed. Once progress is made regarding immunosuppressive therapies and tolerance, envisioning a model where a function can be evaluated without hindering the animals' well-being should be undertaken.

Finally, we recently demonstrated the successful use of this model to test different immunosuppression strategies and better understand the mechanisms behind graft rejection.[35,36] Therefore, this model is proving to be a valuable and relevant preclinical tool in VCA, facilitating the development of effective therapeutic interventions.

CONCLUSIONS

Our study shows the reliability of a modified heterotopic VCA model in pigs with reduced bulkiness but with preserved vascularization of all the components. Moreover, immunologically functioning graft-draining lymph nodes can be incorporated into the graft. Although remaining a complex animal model, taking into consideration our detailed description and the need for a learning curve, we believe our model can be reliably reproduced.

Radu Olariu, MD, PhD
Department of Plastic and Hand Surgery
Inselspital University Hospital
Anna Seiler Haus
Freiburgstrasse 20
3010 Bern, Switzerland
E-mail: radu.olariu@insel.ch

DISCLOSURES

The authors have no financial interest to declare in relation to the content of this article. This project is funded by The Swiss National Science Foundation, Project 32003B_179504.

REFERENCES

1. Petruzzo P, Sardu C, Lanzetta M, et al. Report (2017) of the International Registry on Hand and Composite Tissue Allotransplantation (IRHCTT). *Curr Transplant Rep.* 2017;4:294–303.
2. Diep GK, Berman ZP, Alfonso AR, et al. The 2020 facial transplantation update: a 15-year compendium. *Plast Reconstr Surg Glob Open.* 2021;9:e3586.
3. Wells MW, Rampazzo A, Papay F, et al. Two decades of hand transplantation: a systematic review of outcomes. *Ann Plast Surg.* 2022;88:335–344.
4. Petruzzo P. IRHCTT update: upper extremity and face transplantation. Paper presented at: 15th Congress of the International Society for Vascularized Composite Allotransplantation; June 4, 2022; Cancun, Mexico.
5. Milek D, Reed LT, Echternacht SR, et al. A systematic review of the reported complications related to facial and upper extremity vascularized composite allotransplantation. *J Surg Res.* 2023;281:164–175.
6. Chapman JR, Webster AC, Wong G. Cancer in the transplant recipient. *Cold Spring Harb Perspect Med.* 2013;3:a015677.
7. Ben Brahim B, Arenas Hoyos I, Zhang L, et al. Tacrolimus-loaded drug delivery systems in vascularized composite allotransplantation: lessons and opportunities for local immunosuppression. *Transplantation.* 2024. [Published online ahead of print.]
8. Dhayani A, Kalita S, Mahato M, et al. Biomaterials for topical and transdermal drug delivery in reconstructive transplantation. *Nanomedicine (London, England).* 2019;14:2713–2733.
9. Huelsboemer L, Boroumand S, Kochen A, et al. Immunosuppressive strategies in face and hand transplantation: a comprehensive systematic review of current therapy regimens and outcomes. *Front Transplant.* 2024;3:1366243.
10. Gajanayake T, Olariu R, Leclere FM, et al. A single localized dose of enzyme-responsive hydrogel improves long-term survival of a vascularized composite allograft. *Sci Transl Med.* 2014;6:249ra110.
11. Olariu R, Denoyelle J, Leclère FM, et al. Intra-graft injection of tacrolimus promotes survival of vascularized composite allotransplantation. *J Surg Res.* 2017;218:49–57.
12. Dzhonova D, Olariu R, Leckenby J, et al. Local release of tacrolimus from hydrogel-based drug delivery system is controlled by inflammatory enzymes in vivo and can be monitored noninvasively using in vivo imaging. *PLoS One.* 2018;13:e0203409.
13. Dzhonova DV, Olariu R, Leckenby J, et al. Local injections of tacrolimus-loaded hydrogel reduce systemic immunosuppression-related toxicity in vascularized composite allotransplantation. *Transplantation.* 2018;102:1684–1694.

14. Fries CA, Tuder DW, Davis MR. Preclinical models in vascularized composite allotransplantation. *Curr Transplant Rep*. 2015;2:284–289.
15. Ibrahim Z, Busch J, Awwad M, et al. Selected physiologic compatibilities and incompatibilities between human and porcine organ systems. *Xenotransplantation*. 2006;13:488–499.
16. Üstüner ET, Zdichavsky M, Ren X, et al. Long-term composite tissue allograft survival in a porcine model with cyclosporine/mycophenolate mofetil therapy. *Transplantation*. 1998;66:1581–1587.
17. Üstüner ET, Majzoub RK, Ren X, et al. Swine composite tissue allotransplant model for preclinical hand transplant studies. *Microsurgery*. 2000;20:400–406.
18. Fries CA, Villamaria CY, Spencer JR, et al. A porcine orthotopic forelimb vascularized composite allotransplantation model: technical considerations and translational implications. *Plast Reconstr Surg*. 2016;138:461e–471e.
19. Lee WPA, Rubin JP, Cober S, et al. Use of swine model in transplantation of vascularized skeletal tissue allografts. *Transplant Proc*. 1998;30:2743–2745.
20. Mathes DW, Randolph MA, Solari MG, et al. Split tolerance to a composite tissue allograft in a swine model. *Transplantation*. 2003;75:25–31.
21. Ibrahim Z, Cooney DS, Shores JT, et al. A modified heterotopic swine hind limb transplant model for translational vascularized composite allotransplantation (VCA) research. *J Vis Exp*. 2013;80:e50475.
22. Kuo YR, Sacks JM, Lee WPA, et al. Porcine heterotopic composite tissue allograft transplantation using a large animal model for preclinical studies. *Chang Gung Med J*. 2006;29:268–274.
23. Sun JA, Adil A, Biniazan F, et al. Immunogenicity and tolerance induction in vascularized composite allotransplantation. *Front Transplant*. 2024;3:1350546.
24. Fisher JD, Zhang W, Balmert SC, et al. In situ recruitment of regulatory T cells promotes donor-specific tolerance in vascularized composite allotransplantation. *Sci Adv*. 2020;6:eaax8429.
25. Lese I, Leclère FM, Gayanayake T, et al. Regional lymphatic inclusion in orthotopic hindlimb transplantation: establishment and assessment of feasibility in a rodent model. *Transplant Direct*. 2020;6:e592.
26. Cui Y, Liu K, Monzon-Medina ME, et al. Therapeutic lymphangiogenesis ameliorates established acute lung allograft rejection. *J Clin Invest*. 2015;125:4255–4268.
27. Olariu R, Tsai C, Abd El Hafez M, et al. Presence of donor lymph nodes within vascularized composite allotransplantation ameliorates VEGF-C-mediated lymphangiogenesis and delays the onset of acute rejection. *Transplantation*. 2021;105:1747–1759.
28. Etra JW, Grzelak MJ, Fidder SAJ, et al. A skin rejection grading system for vascularized composite allotransplantation in a preclinical large animal model. *Transplantation*. 2019;103:1385–1391.
29. Cendales LC, Kanitakis J, Schneeberger S, et al. The Banff 2007 Working classification of skin-containing composite tissue allograft pathology: Banff CTA Allograft Pathology Classification. *Am J Transplant*. 2008;8:1396–1400.
30. Fries CA, Lawson SD, Wang LC, et al. Graft-implanted, enzyme responsive, tacrolimus-eluting hydrogel enables long-term survival of orthotopic porcine limb vascularized composite allografts: a proof of concept study. *PLoS One*. 2019;14:e0210914.
31. Ravindra KV, Xu H, Bozulic LD, et al. The need for inducing tolerance in vascularized composite allotransplantation. *Clin Dev Immunol*. 2012;2012:1–11.
32. Zhang C, Merana GR, Harris-Tryon T, et al. Skin immunity: dissecting the complex biology of our body's outer barrier. *Mucosal Immunol*. 2022;15:551–561.
33. Robbins NL, Wordsworth MJ, Parida BK, et al. Is skin the most allogenic tissue in vascularized composite allotransplantation and a valid monitor of the deeper tissues? *Plast Reconstr Surg*. 2019;143:880e–886e.
34. Howsare M, Jones CM, Ramirez AM. Immunosuppression maintenance in vascularized composite allotransplantation: what is just right? *Curr Opin Organ Transplant*. 2017;22:463–469.
35. Arenas Hoyos I, Helmer A, Yerly A, et al. A local drug delivery system prolongs graft survival by dampening T cell infiltration and neutrophil extracellular trap formation in vascularized composite allografts. *Front Immunol*. 2024;15:1387945.
36. Zhang L, Arenas Hoyos I, Helmer A, et al. Transcriptome profiling of immune rejection mechanisms in a porcine vascularized composite allotransplantation model. *Front Immunol*. 2024;15:1390163.